Journal of Nuclear Materials 390–391 (2009) 192–195

Contents lists available at ScienceDirect

Journal of Nuclear Materials

journal homepage: www.elsevier.com/locate/jnucmat

Coupled plasma–wall modeling

A.Yu. Pigarov *, S.I. Krasheninnikov

University of California at San Diego, Center for Energy Research, EBU-II, 9500 Gilman Dr., La Jolla, CA 9209-0417, USA

ARTICLE INFO

PACS:
52.25.Tx
52.55.Dy
52.40.Hf
52.65.−y

ABSTRACT

The new time-dependent one-dimensional code WALLPSI to calculate wall temperature, erosion rates, and concentrations of trapped, chemically bonded, absorbed, and mobile hydrogen inside the wall has been developed. To study basic physics processes, WALLPSI is coupled to the 1-D edge plasma transport code EDGE1D. The results of self-consistent plasma–neutrals–wall modeling with WALLPSI/EDGE1D which show strong plasma–wall coupling are presented. Variation of hydrogen inventory in the wall in response to the changing plasma impact is discussed. Oscillatory behavior and thermal instability of plasma in contact with hydrogen saturated wall are modeled.

1. Introduction

Plasma–surface interaction (PSI) processes are crucial for ITER and future magnetic fusion reactors. Important PSI-related issues are: (i) maintaining high performance burning plasma (e.g. density, recycling, and fuel isotope control); (ii) prediction of power load handling; (iii) evaluation of wall erosion and re-deposition, migration of material, wall material mixing; and (iv) assessment of retention and permeation of hydrogen isotopes in wall materials. To address these issues, sophisticated integrated modeling tools are urgently needed.

However, so far the chemistry, retention, and transport of hydrogen isotope species in wall material as well as the dynamics of composition of multi-material surfaces are not well understood and there is very limited experience in the coupled plasma–wall modeling [1,2]. The classical effects of wall pumping and chemical sputtering which are known since long ago and are crucial for recycling and density control in tokamaks have not been modeled self-consistently with hydrogen wall inventory yet. Moreover, recent experiments showed that during long-pulse discharges the wall conditions can change from gas pumping to gas release [3,4] leading to uncontrollable increase in plasma density, formation of X-point MARFE, and degradation of plasma confinement [5]. Simple analytical models [6] highlighted that interaction of plasma with hydrogen saturated wall could cause thermal plasma instability resulting in massive gas desorption from wall and triggering the plasma detachment and MARFE formation.

First continuum codes for hydrogen transport in wall appeared 30 years ago (e.g. DIFFUSE [7]) and, since that time, there was little progress in continuum modeling capability, whereas large amount of new PSI data were obtained in experiments and by Molecular Dynamics simulations.

We developed the wall and plasma–surface interaction (WALLPSI) code to calculate wall temperature, erosion rates, and concentration of absorbed, mobile and trapped particle species in wall materials (Section 2). The code incorporates new approaches: (i) modeling of dynamics and transport of specific traps produced due to chemical bond breaking and of hydrogen inventory in-there, (ii) non-diffusive transport of hydrogen species via convection directed toward the plasma facing surface (PFS) in the implantation region due to nano-voids created by incident particles for a ns or longer timescales, (iii) moving PFS interface, (iv) dependence of diffusion coefficient on hydrogen concentration and on degree of material amorphization, and (v) interface and infrastructure necessary for WALLPSI coupling to plasma transport codes. These approaches allow WALLPSI to simulate more confidently: highly non-equilibrium kinetics of hydrogen, retention and release of hydrogen species from room up to sublimation temperatures, rates for chemical erosion and radiation enhance sublimation (RES), wall pumping via co-deposition, and saturated wall condition for major fusion-related materials.

In the paper we: (i) present results on hydrogen transport and inventory in wall materials (Section 3), (ii) discuss WALLPSI coupling to our EDGE1D code developed to model the 1-D transport of plasma and neutrals (Section 4), and (iii) report on initial WALLPSI/EDGE1D studies of *self-consistent* plasma-wall coupling and featured instabilities (Section 5).

We use acronyms for convective (CN) and diffusive (DF) transport, reactions (RC), implantation region (ImR), plasma facing surface (PFS), coolant facing surface (CFS), and broken bond (BB) traps.

* Corresponding author.
E-mail address: apigarov@uscd.edu (A.Yu. Pigarov).

0022-3115/$ - see front matter © 2009 Published by Elsevier B.V.
doi:10.1016/j.jnucmat.2009.01.165

2. WALLPSI model

WALLPSI considers transport of particles and heat in the wall along coordinate z, the depth into the wall. The model domain includes: PFS at $z = 0$, bulk, and CFS at $z = \delta$. At present, there are two sorts of particles in the wall: hydrogen isotope atom (denoted as h) and atom of base material ($base$). In future we intend to increase the number of particles to simulate multi-isotope gas and multi-material wall. Hydrogen species are: mobile interstitial atoms, hydrogen trapped in various 'stationary' irregularities of the bulk such as vacancy, dislocation, etc; hydrogen adsorbed at PFS and CFS. We also distinguish the case when hydrogen is chemically bonded to the base material atoms in the bulk and at the PFS (e.g. sp^2 and sp^3 bonding in carbon-based materials or covalent bonding in beryllium). In this case the species are associated with 'non-stationary' traps (broken bond traps) created and destructed dynamically by projectile particles. The species associated with base material are: unperturbed lattice atom (lat), atom with broken chemical bond (bb), and mobile recoil atom. The total density of base atoms is fixed and equal to the average density N_{base} of material under consideration. We consider various processes associated with species migration (mig), bond breaking (br), sputtering (spt), destruction (ds), recombinative desorption (rec), and many others. The process can be of two types: thermally activated (th) and caused by collisions with projectile particles (c).

We use the following notation. The three-indices quantity $N^k_{i,j}$ denotes the particle species density, where index k distinguishes particles at the surface ($k = s$) and in the bulk ($k = v$); index i stands for the particle sort, $i = \{h, base\}$; index j denotes the type of particle as mobile ($j = m$), trapped ($j = tr$), or associated with broken bond ($j = bb$). The process denoted by index $n = \{mig, br, spt, ds, rec\}$ is characterized by its frequency $\nu^{i,j,k}_{l,n}$ (or reaction rate coefficient $\alpha^{i,j,k}_{l,n}$), where indices i,j,k have the same meaning as above, index $l = \{th, c\}$ denotes the type. $T(i,j \to i',j')$ denotes rates associated with processes ($th + c$) resulting in transition of the particle species i in region j to the particle species i' in region j'.

At present, WALLPSI solves the system of nine coupled equations: (1) 1-D CN/DF/RC equation for density $N^v_{h,m}$ of mobile hydrogen; (2) 0-D RC equation for hydrogen retained at PFS and CFS, $N^s_{h,m}$ (we consider these species as mobile since particles can migrate along the surface); (3) 1-D CN/RC equation for density of BB-traps $N^v_{base,bb}$; (4) 1-D CN/RC equation for BB-traps filled with hydrogen $N^v_{h,bb}$; (5) 0-D RC equations for $N^s_{base,bb}$ and $N^s_{h,bb}$ at PFS; (6) 1-D CN/RC equation for density $N^v_{h,tr}$ of hydrogen retained in stationary traps (density profile $N_{st}(z)$, hydrogen capacity, and binding energy for these traps are prescribed); (7) 1-D CN/DF/RC equation for density of recoil base atoms $N^v_{base,m}$; (8) 0-D equation for velocity V_{surf} of PFS movement, and (9) 1-D conductive heat transfer equation to calculate the profile of wall temperature $T_{wall}(z,t)$. Further in this section we briefly discuss a few equations, whereas the detailed description will be given in [8].

Equations describing the densities of hydrogen species $j = \{m, tr, bb\}$ in the bulk have the form: $\partial N^v_{h,j}/\partial t = -\partial \Phi_{h,j}/\partial z + S^v_{h,j}(z,t)\delta_{j,m} + \sum_{j'}[1-\delta'_{j,j}]T(j, v \to j', v) - N^v_{h,j}\nu^{h,j,v}_{c,spt} - V_{surf}\partial N^v_{h,j}/\partial z$. Here $\Phi_{h,j} = -\delta_{j,m}D_m\partial N^v_{h,j}/\partial z + N^v_{h,j}V^{conv}_{h,j}$ is the flux (DF + CN), $\delta_{j,m}$ is Kronecker symbol ($\delta_{i,j} = 1$, if $i = j$, and $\delta_{i,j} = 0$, otherwise), $S^v_{h,j}$ is the source of implanted projectile hydrogen atoms, the third term in rhs stands for various transition processes between the species, $V^{conv}_{h,j}$ is convective velocity directed outward ($V^{conv}_{h,j}$<0) due to migration through voids produced by bombardment which we calculated as $V^{conv}_{h,j} = v_{\oplus}\sum_i \Gamma_{prj,i}\theta_i(z)/\Phi_{\oplus}$ where summation is over all projectile particle species i, $\Gamma_{prj,i}$ is incident flux, $\theta_i(z) = 1 - erf(z/\langle R_i\rangle)$, $\langle R_i\rangle$ denotes the penetration range, $v_{\oplus}$ is characteristic velocity at critical flux $\Phi_{\oplus}$ which are the fitting parameters. The boundary condition on $\Phi_{h,j}(z = 0)$ expresses the flux balance at PFS/bulk interface.

Frequencies of thermally activated processes have Arrhenius form: $\nu^{i,j,k}_{th,l} = \nu_l g_l \exp\{E^{i,j,k}_l/[k_B T_{wall}]\}$, where ν_l is typically jump attempt frequency $\nu_{base} = 10^{12}$/s with correction factor g_l, $E^{i,j,k}_l$ is the sum of activation energy and specific heat, k_B is Boltzmann constant. Collisional frequencies are calculated as: $\nu^{i,j,k}_{c,l} = \sum_p J_{prj,p}\sigma^{i,j,k}_l$ where summation is over all projectile species, $J_{prj,p}(z)$ is scalar flux of projectile p at depth z, $\sigma^{i,j,k}_l$ is typically the averaged Thompson-like cross-section with threshold $E^{i,j,k}_l$. We employ the concentration-dependent diffusion coefficient for mobile hydrogen: $D_m = D_{th}[1 + \{U_h/k_B T_{wall}\}C_h\{1 - C_h\}] + D_c$, where $D_l = D^{am}_l\gamma_{am} + D^{orig}_l(1-\gamma_{am})$, $l = \{th, c\}$, γ_{am} is the degree of amorphisation, D^{am}_{th} and D^{orig}_{th} are thermally-activated diffusion coefficients in amorphous and original material state, D_c describes projectile-induced random walk, $D^{i=am,orig}_l \propto \nu^{h,m,v}_{l,mig}$, $U_h < 0$ is the characteristic of H–H interaction energy, $C_h = \sum_j N^v_{h,j}/N_{base}$ is total concentration of hydrogen. This dependence reflects the fact that generally diffusive flux is driven by the gradient of chemical potential which is a function of concentration of species [9]. We kept D_m be positive to avoid instabilities caused by binodal and spinodal decomposition at high concentrations [9].

Equations for hydrogen species $j = \{m, bb\}$ at PFS have the form: $dN^s_{h,j}/dt = \Theta^s_{h,j}S^s_{h,j} - N^s_{h,j}N^s_{h,j}\alpha^{h,j,s}_{th,rec} - N^s_{h,j}\nu^{h,j,s}_{c,rec} - N^s_{h,j}\sum_k \nu^{h,j,s}_{k,ds} + \sum_{j'}\{[1-\delta_{j,j'}]T(j, s \leftrightarrow j', s) + T(j, s \leftrightarrow j', v)\}$, where $S^s_{h,j}$ is the source due to capture of projectile hydrogen species; $\Theta^s_{h,j}$ is surface coverage by unoccupied cites, other terms in rhs describe desorption via Langmuir–Hinshelwood mechanism, Eley–Rideal mechanism, collision-induced and thermal desorption, and transitions.

We also present the equation for density of base atoms with broken bonds: $dN^v_{base,bb}/dt = -[(N^v_{base,bb})_{max} - N^v_{base,bb}]\sum_k \nu^{base,lat,v}_{k,br} - [N^v_{base,bb} - N^v_{h,bb}]\sum_k \nu^{base,bb,v}_{k,ds} + N^v_{h,bb}\sum_k \nu^{h,bb,v}_{h,ds} - N^v_{base,bb}\nu^{base,bb,v}_{c,spt} - \partial N^v_{baee,bb}V^{conv}_{base,bb}/\partial z - V_{surf}\partial N^v_{base,bb}/\partial z$, where the first and second terms describe creation and destruction of BB-traps, the third stands for bond cancellation rates in destruction of traps populated by hydrogen, the fifth term describes convective transport.

To calculate the velocity V_{surf} of plasma facing surface movement, we solve material flux imbalance equation: $N_{base}dz_{surf}/dt = N_{base}V_{surf} = \Gamma_{in,base} - \Gamma_{out,base}$, where $\Gamma_{in,base}$ is the flux of deposited projectile particles (adsorbed and implanted), $\Gamma_{out,base}$ is the flux of ejected particles, which contain base material atoms. Note that groups of incorporated processes causing these ejectiles can be associated with physical and chemical sputtering, RES and thermal sublimation.

The particle and energy reflection coefficients, profile of implanted hydrogen atoms, penetration range, profile of scalar flux of projectiles in matter, distribution of recoil atoms, and sputtering yields were pre-calculated by TRYDIN code [10], averaged over Maxwellian distributions of incident particles, fitted and tabulated.

3. Hydrogen inventory modeling

Consider the build-up of hydrogen inventory starting from virgin wall material (assume graphite). Along with breaking the chemical bonds (production of BB-traps), plasma ions and neutrals impinging the wall with energy E_o also cause amorphization that affects the mobile hydrogen diffusion. For $E > 20$ eV, cross-sections for bond breaking are rather large, so that $N^v_{base,bb}$ and $N^s_{base,bb}$ increase and tend to saturate depending on irradiation dose. Even at room T_{wall} in amorphous state, BB-traps are rapidly populated due to migration of mobile hydrogen atoms because of relatively small reported migration energy. Concentration of hydrogen in BB-traps is measured in some tokamaks showing $N^v_{h,bb}/N_{base} \sim 0.1$–$0.4$ dependent on type of graphite and tile position. To match these numbers we suggest that destruction frequency

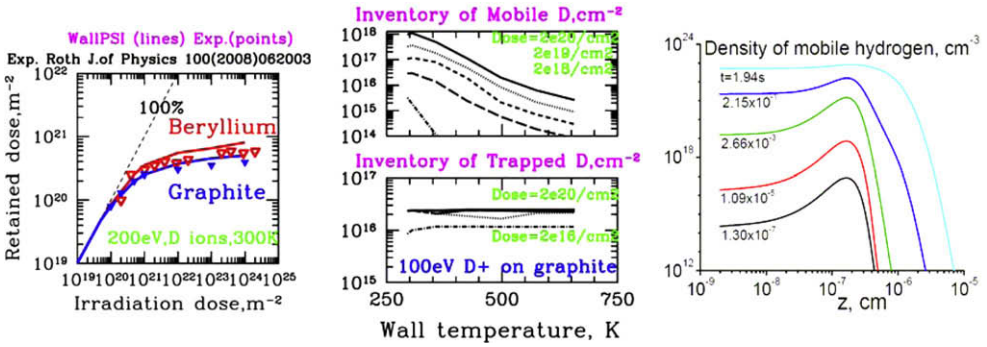

Fig. 1. Comparison of WALLPSI results with experimental data for D retention in graphite (blue) and beryllium (red) is given in left panel. Middle panels display inventory of mobile (top) and BB-trapped (bottom) deuterium as functions of wall temperature (curves correspond to different irradiation doses). Temporal evolution of the profile of mobile D in graphite is shown on right panel. (For interpretation of the references to color in this figure legend, the reader is referred to the web version of this article.)

$\sum_k v_{k,ds}^{base,bb,v} / \sum_k v_{k,br}^{base,lat,v}$ is by factor 3–1.5 larger than BB-trap production.

In experiments reviewed in [11], the retained dose for D in pyrolitic graphite (Fig. 1, left) is consistent with concentration of hydrogen filling BB-traps at 0.4 level and $v_\oplus \sim 10^{-6}$ m/s, $\Phi_\oplus \sim 10^{23}$ m^{-2} s^{-1}. Comparison of WALLPSI with experimental data showing good agreement is given in Fig. 1, left.

As expected, concentration of mobile hydrogen $N_{h,m}^v$ strongly depends on $T_{\rm wall}$. The WALLPSI calculations of mobile $I_m = N_{h,m}^s + \int N_{h,m}^v dz$ and trapped $I_t = N_{h,bb}^s + \int [N_{h,bb}^v + N_{h,tr}^v] dz$ inventories for a graphite wall irradiated by deuterium are displayed on Fig. 1 (middle). Since migration energy of deuterium in amorphous ImR is small ~0.5 eV, I_m practically exponentially decreases with $T_{\rm wall}$ (Fig. 1, top). By contrast, I_t is practically constant for $T_{\rm wall} < 700$ K since C–H bond energy is ~4 eV. I_m has pronounced dependence on incident dose, but not I_t. At low $T_{\rm wall}$ and doses enough for saturation, I_m is substantially larger I_t, providing strong sensitivity of hydrogen output on varying plasma conditions.

At high incident fluxes and low $T_{\rm wall}$ the accumulation of all hydrogen species in ImR up to $C_h \sim 1$ results in substantial decrease in diffusion coefficient and may cause spinodal instability. In this case, the dominant role plays induced convection. This non-diffusive transport limits concentrations of mobile hydrogen at reasonable level $N_{\rm cr}/N_{base} \sim 1/2$ determined by values of prescribed velocity $v_\oplus$ for any incident flux $\Phi > \Phi_\oplus$ as follows from the simplified flux balance: $N_{cr} v_\oplus \Phi/\Phi_\oplus = \Phi(1-\alpha_p)$, α_p is the back-scattering coefficient dependent on projectile energy. Evolution of profile of mobile hydrogen for graphite irradiation by 100 eV D+ is shown on Fig. 1, right. As seen, in about two seconds, the concentration of mobile particles tends to become flat over ImR and determines the saturation level.

4. EDGE1D plasma model

EDGE1D model mimics the 1-D cross-field transport of plasma and neutral gas in tokamaks. The system of five coupled equations is given to calculate the profiles of plasma (n) and neutral gas (N) densities; electron (T_e), ion (T_i) and neutral gas (T_N) temperatures. Periodic boundary conditions are assumed at $x = 0$. Plasma is transported along coordinate x from source region ($0 < x < \Delta$) to the wall at $x = L$. The plasma particle ($G_{\rm ext}$) and power (W_e and W_i) inputs are uniformly distributed over $0 < x < \Delta$. The gas evacuation time in the SOL ($\Delta < x < L$) is $\tau_{\rm pump}$. Continuity equations are given for plasma $\partial n/\partial t = -\partial \Phi_p/\partial x + G_{\rm ext} + G_{\rm col}$, and neutrals $\partial N/\partial t = -\partial \Phi_N/\partial x - N/\tau_{\rm pump} - G_{\rm col}$, where $\Phi_p = nV_c - D_p \partial n/\partial x$ and $\Phi_N = -(D_N/T_i)\partial N T_N/\partial x$ are fluxes; $G_{col} = K_{ion} nN - K_{rec} n^2$, $D_N = T_i/[M_i n(K_{ion} + K_{rec} n/N + K_{cx})]$, M_i is the mass of ion; D_p and V_c are the prescribed cross-field diffusion coefficient and convective velocity of plasma ions; K_{ion}, K_{rec}, and K_{cx} denote the rate coefficients, respectively, for hydrogen ionization, recombination, and charge exchange processes. Heat transfer is described by the set of equations for $j = \{i,e,N\}$: $\partial E_j/\partial t = -\partial Q_j/\partial x - \Theta_j + \Pi_j + W_j$, where $E_j = 3n_j T_j/2$, $Q_j = q_j + 5\Phi_j T_j/2$, $q_j = -\lambda_j \partial T_j \partial x$, $\lambda_j = 3n_j \chi_j/2$, $\Pi_j = \{\Phi_j/n\}\partial n T_j/\partial x$; $n_{(j=N)} = N$. Sink terms are $\Theta_e = Q_{ei} + L_{imp} n^2 + L_{rad} nN + I_o G_{\rm col}$, $\Theta_i = Q_{iN} - Q_{ei} + Q_{\rm col}$, $\Theta_N = -Q_{iN} - Q_{eN}$, $Q_{col} = E_i K_{rec} n - E_N K_{ion} n$, $Q_{iN} = K_{cx}(NE_i - nE_N)$, L_{imp} and L_{rad} are radiation loss rates for impurity and hydrogen atoms which depend on plasma parameters; $I_o = 13.6$ eV; $Q_{ei} = (T_e - T_i)\varphi_{ei}$ describes energy exchange via Coloumb collisions. We assume that impurity concentration is the fixed fraction ζ_{imp} of plasma density.

At the plasma–wall interface, $x = L$, we use the following boundary conditions: $\Phi_p = nC_{sh}$, $\Phi_N = \Gamma_{N,in} - \alpha_p \Phi_p - \Gamma_{N,out}$, $Q_e = \gamma_e T_e n C_{sh}$, $Q_i = \gamma_i T_i n C_{sh}$, $Q_N = W_{N,in} - E_{N,p}\Phi_p - W_{N,out}$, where $\Gamma_{N,in} = NC_N/4$ is the flux of atoms on wall, C_N is the thermal velocity of Maxwellian atoms, and C_s is the ion sound speed, γ denotes heat transmission factor, $C_{sh} = C_s \sin(\iota)$, ι is the angle between the wall and magnetic field line. When coupled, EDGE1D passes the influxes whereas WALLPSI returns the outfluxes and α_p.

In WALLPSI/EDGE1D modeling we consider input parameters close to those in DIII-D tokamak: $L = 0.4$ m, $\Delta = 0.1$ m, $W_e = W_i = 1.2$ MJ/m^3. We prescribe the profiles to anomalous cross-field plasma transport coefficients $P = \{D_p, \chi, V_c\}$ in the power law form: $P = A$, for $0 < x < \Delta$, and $P = A + (B - A)\ [(x-\Delta)/(L-\Delta)]^\beta$, for $\Delta < x < L$. We assume $\zeta_{imp} = 0.05$ and that the transport is rather fast: $A_D = B_D = 1$ m^2/s; $A_V = 10^{-4}$, $B_V = 1$ m/s; $A_\chi = 0.3$, $B_\chi = 1$ m^2/s, $\beta = 8$ and provide plasma profiles close to those observed in DIII-D edge. Calculations were done for deuterium and graphite wall.

5. Coupled plasma–wall modeling

In EDGE1D, the plasma particle balance is determined by ion source $G_{\rm srs} = G_{\rm ext}\Delta$, volumetric gas pumping $G_{\rm pump} = \int N/\tau_{\rm pump} dx$, and wall pumping $G_{\rm wal} = (1-\alpha_p)\Phi_p + \Gamma_{N,in} - \Gamma_{N,out}$. Initial plasma profiles are obtained running EDGE1D to steady state (~1 s) assuming fixed recycling coefficient $\alpha = 0.9$ ($\alpha_p = \alpha$, $\Gamma_{N,out} = \alpha\Gamma_{N,in}$) for given $\tau_{\rm pump}$ and $G_{\rm srs} = 5 \times 10^{20}$ m^{-2} s^{-1}. Then we start self-consistent WALLPSI/EDGE1D iterations studying the plasma parameter evolution during discharge with several seconds duration $T_{\rm dis}$. Total particle exhaust rate $G_{\rm exh} = G_{\rm pump} + G_{\rm wal}$ is strong non-linear function of edge plasma parameters. $G_{\rm wal}$ depends on incident plasma flux Φ_p, energy of projectile particles, and wall inventory; whereas $G_{\rm pump}$ depends on neutral density profile. When wall is far from saturation, it can be the dominant hydrogen sink retaining almost 100% of implanted flux, however initial flux $\Phi_p \sim 10^{21}$ m^{-2} s^{-1} is large and can saturate the wall in time $t < T_{\rm dis}$. In the case

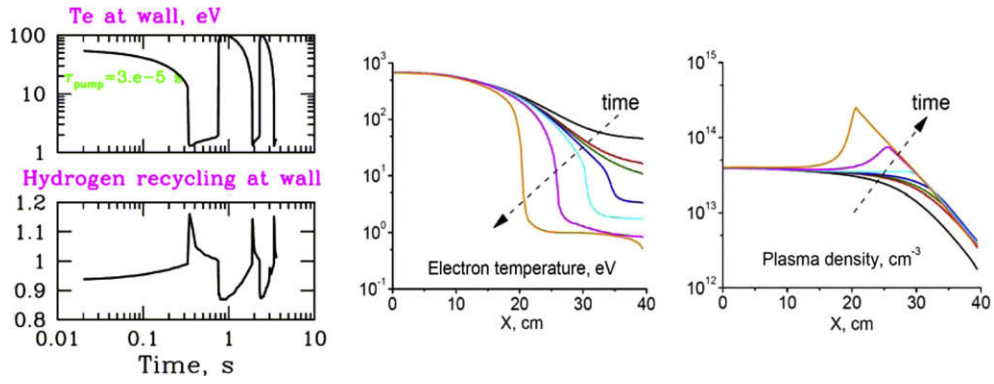

Fig. 2. Temporal variation of plasma temperature near the wall (left top panel) and of deuterium recycling coefficient (left bottom). Evolution of plasma temperature (middle panel) and density (right) profiles corresponding to the MARFE-like collapse of edge plasma $20 < x < 40$ cm.

when $\tau_{\rm pump} < 10^{-6}$ s is extremely small, $G_{\rm exh} > G_{\rm srs}$ during $T_{\rm dis}$ and discharge ends with the low density and the high temperature which has rather flat profile. For $10^{-6} < \tau_{\rm pump} < 3 \times 10^{-5}$ s, Φ_p is not decreasing and the wall due to continuous irradiation has time to saturate (in a way shown in Fig. 1, right). In saturation phase, wall pumping gradually decreases and plasma parameters vary slowly (for example, when calculating for $t > T_{\rm dis}$ for $\tau_{\rm pump} \sim 10^{-5}$ s, edge T_e decreases from 80 eV to 20 eV during 100 s). For $\tau_{\rm pump} \sim 3 \times 10^{-5}$ s, we observed oscillatory dynamics in plasma parameters and wall inventory when hydrogen atoms released from the wall are pumped in plasma. Decreasing $\tau_{\rm pump}$, oscillations increase in amplitude and correspond to abrupt crashes of edge plasma (see Fig. 2, left). Here 10–20% variation in recycling coefficient corresponds to transition between detached and hot sheath limited edge plasmas. The positive loop between release of hydrogen and increased heat/particle fluxes can trigger the thermal instability [6]. When we start with saturated wall conditions (i.e. initially high I_m), the plasma parameter evolution typically ends in MARFE-like collapse as shown in Fig. 2, middle-right panels, with formation of low temperature ($\sim$1 eV) high density ($\sim 10^{20}$/m^3) plasma zone separating the core plasma and wall. Position of this zone (ionization front) depends on plasma power/particle inputs and transport coefficients. For $\tau_{\rm pump} > 10^{-4}$ s, the particle exhaust is so slow that the positive imbalance condition ($G_{\rm srs} > G_{\rm exh}$) is quickly reached and is followed by the MARFE-like collapse and uncontrollable plasma density increase in the core region.

6. Conclusions

At low temperatures, an important role in mobile hydrogen transport plays induced outward convection. When diffusion is relatively slow, the convection velocity $V^{conv}_{h,m} \propto v_\oplus \Phi/\Phi_\oplus$, $v_\oplus \sim 10^{-6}$ m/s, limits the concentration $N^v_{h,m}$ for any incident flux $\Phi > \Phi_\oplus \sim 10^{23}$ m^{-2} s^{-1} at the level $N^v_{h,m}/N_{base} \sim 1/2$. This approach is reasonable replacement to the local mixing model [12]. At low wall temperatures, concentrations of mobile hydrogen in the implantation region (ImR) can be large (for C and Be) and even exceed concentrations of trapped hydrogen. Mobile hydrogen can easily leave ImR in heating or sputtering and affect strongly edge plasma parameters, whereas trapped hydrogen can be released only at very high temperatures >1000 °C causing tritium-related safety problems in fusion reactors. Experiments are needed for evaluation of mobile hydrogen inventory and for further validation of WALLPSI model.

The coupled WALLPSI/EDGE1D modeling showed that hydrogen wall inventory build-up in some materials results in very high values of recycling coefficient or even >1 and causes without external stabilizing loop the MARFE-like crash of edge plasma. The modeled transitional effects include oscillations due to switching from wall pumping to gas release. Thermal instability of plasma caused by intense release of hydrogen from wall has been identified theoretically and modeled here and its detailed analysis will be reported elsewhere.

WALLPSI is a part of more sophisticated SciDAC project on Framework Application for Core–Edge Transport Simulations (FACETS) [13]. Initially this work includes coupling of core plasma codes, 2-D edge-plasma code UEDGE, and WALLPSI. The project goal is to provide detailed core–edge–wall transport modeling of tokamak fusion reactors.

References

[1] J.T. Hogan et al., J. Nucl. Mater. 241 (1997) 612.
[2] M. Siguhara et al., J. Nucl. Mater. 266 (1999) 691.
[3] T. Loarer et al., Nucl. Fus. 47 (2007) 1112.
[4] E. Tsitrone et al., J. Nucl. Mater. 363–365 (2007) 12.
[5] H. Takenaga et al., J. Nucl. Mater. 337–339 (2005) 802.
[6] S.I. Krasheninnikov et al., Phys. Plasmas 13 (2006) 094502.
[7] M.I. Baskes et al., J. Nucl. Mater. 112&113 (1982) 663.
[8] A.Yu. Pigarov, S.I. Krasheninnikov, Phys. Plasmas, submitted for publication.
[9] L.I. Smirnov, Int. J. Hydrogen Energy 24 (1999) 813.
[10] W. Eckstein, Computer Simulations of Ion–Solid Interaction, Springer, Berlin, 1991.
[11] J. Roth, J. Phys. 100 (2008) 062003.
[12] D.K. Brice et al., J. Nucl. Mater. 111&112 (1982) 598.
[13] J.R. Cary et al., J. Phys. 78 (2007) 012086.